CFD Study of Unsteady Flow Through Savonius Wind Turbine Clusters

Mohamed Meziane*‡, Elhachmi Essadiqi**, Mustapha Faqir**, Mohamad Fathi Ghanameh**

* Condensed Matter and Renewable Energy Laboratory, Faculty of Science and Technology, Hassan II University of Casablanca, Morocco

** Université Internationale de Rabat, AERO School, LERMA Laboratoy, Rocade Rabat-Salé, 11100 Sala el Jadida, Morocco.

(mezian.med@gmail.com, mustpha.faqir@uir.ac.ma, elhachmi.essadiqi@uir.ac.ma, fathi.ghannmeh@uir.ac.ma)

‡Corresponding Author; Mohamed Meziane, Tel: +212 6 42 88 52 14,

mezian.med@gmail.com

Received: 04.01.2019 Accepted:29.01.2019

Abstract- The interaction between Savonius vertical axis wind turbine clusters installed in far or close proximity can devalue or enhance the output power of single Savonius vertical axis wind turbines. In this paper, the effect of spatial distribution is studied for the development of efficient Savonius vertical axis wind turbine farms. Numerical simulations are performed for a single Savonius wind turbine, sets of two rotating turbines in three different configurations (aligned, parallel and oblique configurations), and clusters of three rotating turbines, using five separation distances of 0.25D, 0.5D, 1D, 1.5D and 2D, making a total of twenty-two test scenarios. The commercial Computational Fluid Dynamics (CFD) software Fluent 15.0 is used for the numerical study. The torque and power coefficient results of single Savonius turbine are compared and validated against experimental and numerical data based on the literature review. The results showed that there was a combined effect related to the inter-turbine distance and the output power. This combined effect showed an efficient three Savonius turbine cluster having an average power coefficient 3 times higher than an isolated turbine. Best Savonius farm efficiency and high output power could be obtained by considering, at least, these two parameters.

Keywords Wind energy, Vertical axis wind turbines, CFD simulation, Savonius interaction, wind farms.

1. Introduction

Wind energy proves to be an alternative to fossil and nuclear energies based on efficiency [1-6]. The most efficient wind energy harvesting method consists in the use of horizontal axis wind turbines (HAWTs), that in the last years have been developing towards larger diameters (up to 160 m) and larger power production (up to 10 MW). After research studies on horizontal-axis wind turbines, which dominate the majority of the wind energy industry because of their higher efficiency, compared to vertical-axis wind turbines (VAWTs) [7-10]. Recently, vertical axis wind turbines have been receiving increasing interest. They are seen as a good candidate for installation in urban areas [11] and also as a potential candidate for the future of large-scale offshore wind turbines [12-14]. VAWTs can be classified into two categories: lift devices technology (Darrieus turbines), and drag devices technology (Savonius turbines). This type of wind turbines can operate under wind from any direction and is particularly advantageous for its lesser maintenance requirement, easier assembling, cheaper installation, and lesser aerodynamic noise [15-18]. In this present paper, a numerical simulation of the interaction between adjacent Savonius vertical axis wind turbine was conducted for renewable energy generation. This wind turbine is a simple device, designed by cutting a cylinder into halves, along its central axis and relocating the semi cylindrical surfaces sideways. The outlook of this turbine is analogous to an « S » when viewed from the top. These turbines are designed to be driven by the wind drag force and their peak power efficiency can reach up to 30% [18, 19].

Experimental investigations have been carried out to improve the performance of Savonius vertical axis wind turbine by studying the effect of the number of blades, blade overlap, overlap ratio, gap width, shape of the blade and reduction of the anti-rotation torque of the rotor shaft using curtains or ducts [20-24].

Sukanta Roy et al. [25] proposed a differential evolution algorithm based on inverse methodology to optimize the overall dimensions of a Savonius wind turbine with semicircular blades. The interaction between multiple Savonius wind turbines implemented in close proximity enhances their performance [26]. This interaction is a function of the gap distance, relative direction of rotation and relative phase angle between the rotors.

To investigate the flow evolution around Savonius wind turbines and estimate their efficiency, some recent studies [27-30] take advantages of CFD simulations. In a recent work done by Shaheen et al. [31] a cluster of Savonius triangular farms was developed using the enhanced three co-rotating triangular turbine cluster developed in their previous study [32]. Triangular clusters of three Savonius wind turbines are studied to obtain the optimum gap distance and oblique [32]. The performance of the clusters showed an enhancement in the average power coefficient up to 34% relative to an isolated turbine of power coefficient. The effect of modifying the Savonius rotor blade showed that the modification of the blades of the rotor causes an increase of the rotor performance [33]. Effect of spacing between four hydraulic Savonius rotors was studied [34] and it is found that the rotors at the rear have higher rpm and that maximum energy capture takes place for minimum spacing between the rotors. Recent other studies have been performed to assess the performance of lift-driven VAWTs [35, 36] and drag-driven Savonius [37] turbines using experimental and CFD approaches.

In this present work, Savonius wind turbine farms are studied using the enhanced two-turbine-cluster. The two Savonius turbines cluster with a gap distance of 0.5D having an average power coefficient 2 times higher than an isolated turbine. Numerical simulations of farms that consist of three backward and forward configurations confirm the enhancement and the pattern progression for larger farms.

Nomenclature

rpm	rotation per minute
δ	overlap ratio
e	overlap distance
D	overlap diameter
D_0	rotating zone diameter
ρ	air density
V	free stream velocity
A	swept area of the turbine
TSR	tip speed ratio
CFL	Courant-Friedrichs-Lewy condition
ω	rotational speed of the turbine
$P_{turbine}$	power produced by the turbine,
P_{wind}	power available in the wind
T	torque acting on the turbine
C_T	torque coefficient
C_P	power coefficient
μ	Dynamic viscosity
u	Instantaneous velocity
$\bar{u}$	Mean velocity
u′	Fluctuating velocity
$\bar{f}_i$	Body forces
$\bar{S}_{ij}$	Mean rate of strain tensor.

2. Numerical Model

2.1. Computational domain and boundary conditions

Fig.1 shows the geometry of two-bladed semi circular Savonius wind turbine used on this 2D unsteady simulation, where the overlap distance ‘e’ corresponds to the distance between two buckets, D is the overlap diameter of Savonius turbine and D0 is the diameter of the rotating zone (see Fig. 1). The power coefficient of two bladed turbines is about 1.5 times higher than the three bladed turbines [38]. The overlap ratio corresponds to the distance between the turbine blades, divided by the blade chord length and is given by □□= 0.20. The Savonius turbine of this work founded in reference [25] and its dimensions are listed in the Table 1.

The computational domain is divided into two sub-domains; a circular moving zone containing the turbine, rotating with the same angular velocity of the rotor (zone 1)

and a rectangular fixed zone, determining the overall domain extent (zone 2). The dimensions of the rectangular zone are selected in such a way that the results are not affected by the boundaries of the domain. The main dimensions of the fixed zone are shown in Fig.2. The connectivity between the two separated regions as well as the relative motion of the velocity components is guaranteed by a circular sliding interface. The rotating region is placed at a distance 3D from the upper and lower sides of the domain, where a symmetry condition was assigned. The inlet velocity of 6.2 m/s and pressure outlet boundary conditions were placed respectively at a 4D distance upwind and 6D distance downwind with respect to the rotational axis of the turbine. The blades are considered to be a no slip wall in reference to a moving fluid zone. The same domain features are used for the simulation of the two and three turbine cluster turbine farms,

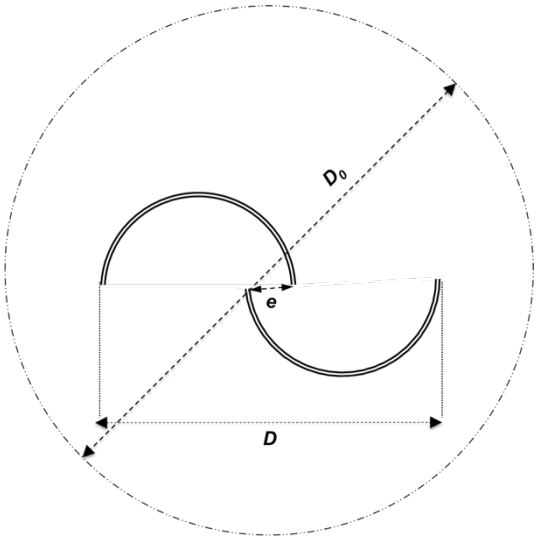

Fig. 1. Two bucket Savonius vertical axis turbine

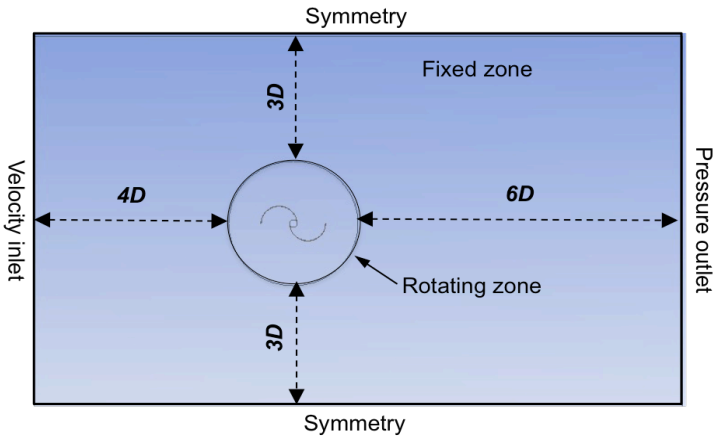

Fig. 2. Computational domain

The performance of the Savonius wind turbine is estimated in terms of the following equations:

$$C_T = \frac{T}{0.5\,\rho A V^2 R}$$

$$C_P = \frac{P_{turbine}}{P_{Wind}} = \frac{T\,\omega}{0.5\,\rho A V^3} = TSR.\,C_T$$

2.2. Domain discretization and mesh sensitivity study:

Fig.3a shows the mesh distribution near the blade. The finite volume method is used to transform the fluid dynamics partial differential equations into a set of algebraic equations, which is solved by iterative methods. Fig.3b shows a close view of the mesh in the vicinity of the rotating region. An inflation of 12 levels of quad cells is imposed to adjust a fine boundary layer near the blade with first layer thickness of 4 10^{-5} m and the increment ratio of 1.12.

Table 1. Dimensions of the Savonius wind turbine

Turbine type	Savonius wind turbine
Number of buckets	2.0
Blade diameter (m)	0.21
Buckets diameter (m)	0.105
Overlap ratio	0.20

Fig.4 shows the y+ variations at two different rotation angle. In order to capture the flow properties at the vicinity of the blade, an average y+ value less than 1 can be observed in this

observed in the torque coefficients of the different rotors. Fig.4. A mesh sensitivity study is performed for all simulations. Six mesh independent tests have been carried out until there is no significant change

The number of cells is shown in Table 2. From 190 000

elements we remark that the torque coefficient value remains stable and its value is in good agreement with the results found by Sukanta [21]. The same mesh topology is repeated for the two and three turbine farm simulations. For mesh convergence, $CFL = Vdt/dx$ close to 1 is ensured.

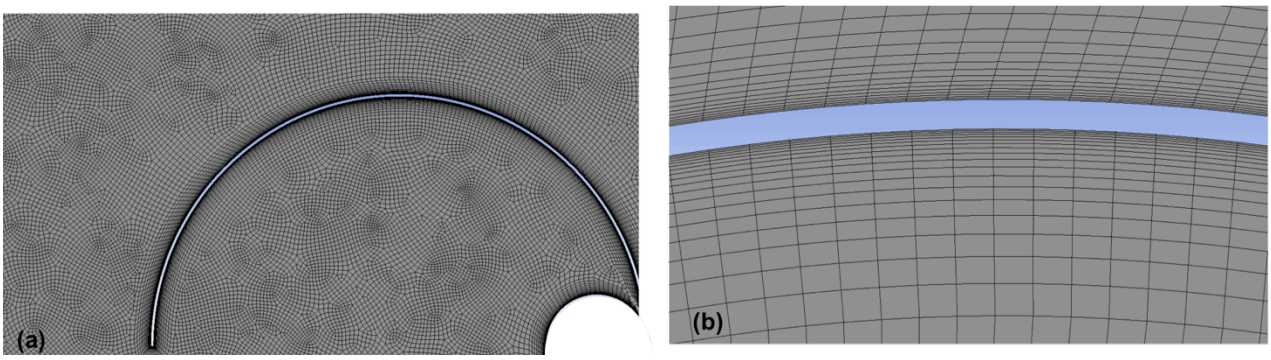

Fig.3. Mesh distribution near the blade

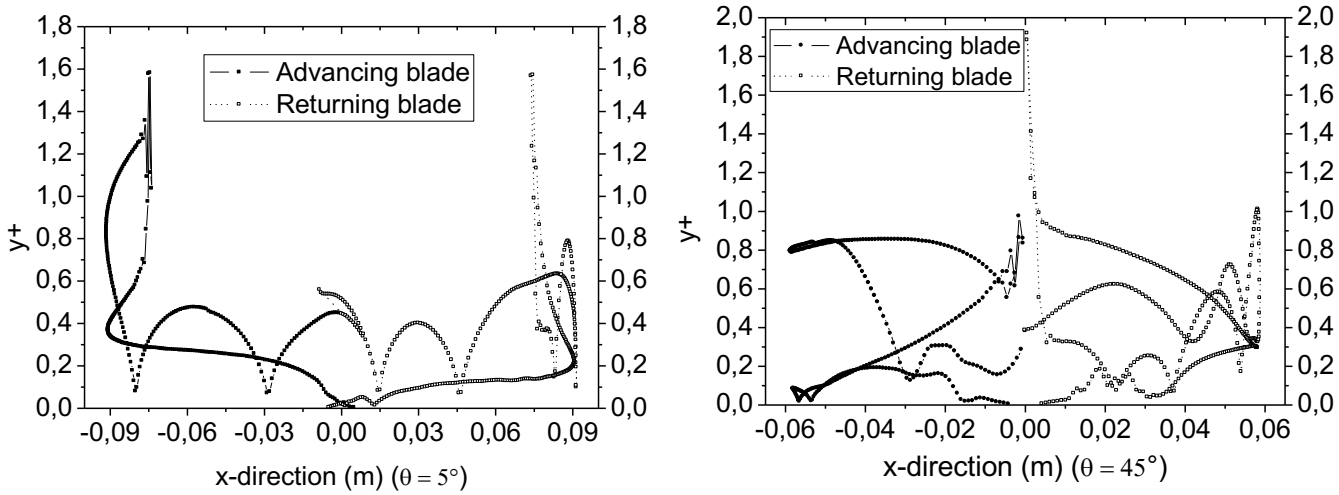

Fig.4. Y+ on the turbine blades at θ = 5° and θ = 45°

Table 2. Mesh refinement for single Savonius turbine.

Mesh level	Number of cells	C_m	C_p
1	35 000	0.282	0.226
2	54 000	0.304	0.243
3	90 000	0.347	0.278
4	190 000	0.357	0.286
5	290 000	0.355	0.284
6	500 000	0.357	0.286

3. Numerical Simulation Model

In this present paper, the results are obtained by applying the finite volume method to solve the unsteady Reynolds average Navier-Stokes equations using Fluent code [39, 40]. These equations are given as follows :

$$\rho\bar{u}_j \frac{\partial \bar{u}_i}{\partial x_j} = \rho\bar{f}_i + \frac{\partial}{\partial x_j}\left[-\bar{p}\,\delta_{ij} + 2\mu\bar{S}_{ij} - \overline{\rho u_i' u_i'}\right]$$

Where, $\bar{S}_{ij} = \frac{1}{2}\left(\frac{\partial \bar{u}_i}{\partial x_j} + \frac{\partial \bar{u}_j}{\partial x_i}\right)$

To achieve a good resolution, these equations are solved using SIMPLE method with the second order upwind scheme for the spatial discretization for momentum, energy and turbulence equations, as well as the second order fully implicit for the time differencing. For the solution iteration, the time step size is taken as 1 10^{-4} corresponding to 1° revolution and the number of iterations per time step is 30. The simulations are run for 10 complete revolution cycles of the turbine.

The choice of turbulence models plays an important role to capture the correct solution. However, each of the turbulence models has their own advantages and disadvantages. In this paper, standard k-ε turbulence model and SST k-ω turbulence model are tested to predict the flow field over Savonius wind turbine with overlap δ = 0.20. The inlet velocity is equal to 6.2 m/s and TSR is given as 0.8. The average C_T and C_P are compared with the experimental study of Sukanta et al. [25] and Blackwell et al. [38]. Fig.5 show the results of torque coefficient variation at different time steps, using standard k-ε turbulence model and SST k-ω turbulence model.

4. Results

4.1. Validation of single Savonius wind turbine

The variation of average torque coefficient of single Savonius turbine at different time steps is calculated at tip speed ratio of 0.8. Fig.5 shows this variation during 10 complete revolution cycles using standard k-ε turbulence model and SST k-ω turbulence model. It is observed that after the third period, it follows almost a cyclic path, and hence, averaged to give a more accurate value.

The influence of cell number on the choice of turbulence model is shown in Fig.6. The average torque coefficient increases as number of cells increases, and achieves its correct value (C_T = 0.355) very early in the case of SST k-ω turbulence model compared to standard k-ε turbulence model. The value of average torque coefficient is in good agrement with experimental and numerical data [25, 39]. The SST k-ω turbulence model is more appropriate, it is due to fact that this model is a blended model of k-ω and k-ε turbulence models, comprising the benefits of near wall and free stream compabilities. The SST k-ω turbulence model is adopted in this study.

The k-ω model is an empirical model based on model transport equations for the turbulence kinetic energy (k) and the specific dissipation rate (ω), which incorporates modifications for Low- Reynolds-Number effects, compressibility, and shear flow spreading [41].

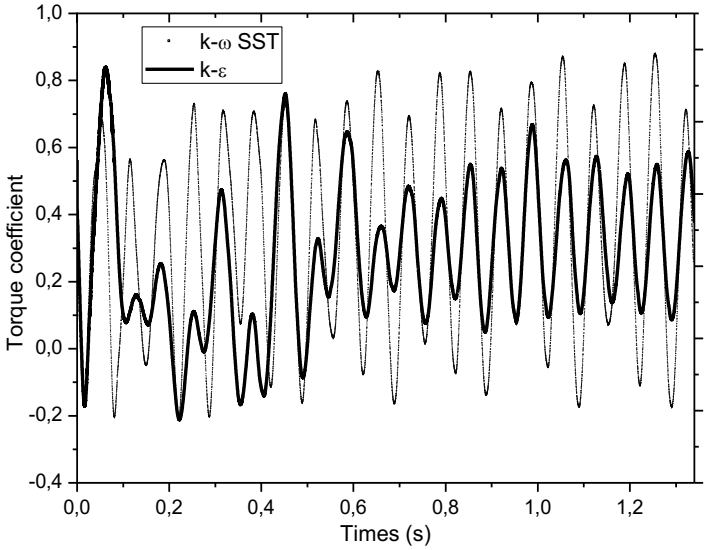

Fig.5. Variation of torque coefficient at different time steps

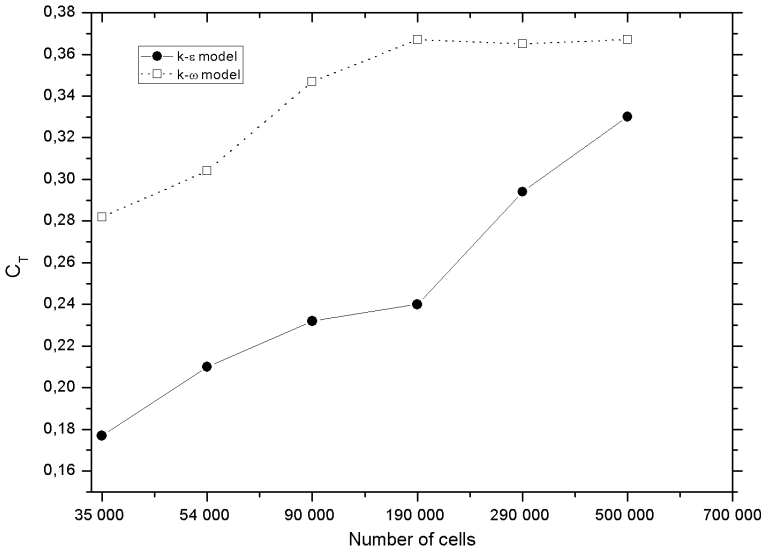

Fig. 6. Comparative study of various turbulence models at different time intervals

Fig.7 and 8 show the velocity vector and pressure distribution at two different time steps for single Savonius turbine with □□= 0.20. Different kinds of flow phenomena

are observed around the blades during their rotation. The momentum transfered to the blades on the curved surfaces by the air flow particles causes the rotation. The curved blades are aligned so that there is always a directional flow striking the concaved surfaces. The curvature of the blades helps in capturing the maximum kinetic energy from the orbiting air flow particles. At t = 1.31s (corresponding to 9 complete revolutions and 270°), the Coanda effect is observed on the concave surface of the advancing blade (blade 2), and a pressure difference appears between the concave and convex sides of the same blade. Simultaneously, a flow separation takes place on the returning blade (blade 1) which causes the vortices and dead zones. In contrast, at t = 1.34s (corresponding to 10 complete revolutions), the Coanda effect and pressure difference move to the returning blade and the flow separation appears on the advancing one.

Flow separation and vortices are observed near to the tip and are responsible to reduce the performance of the Savonius turbine. Hence, the pressure difference contribute to the lift force of the blade.

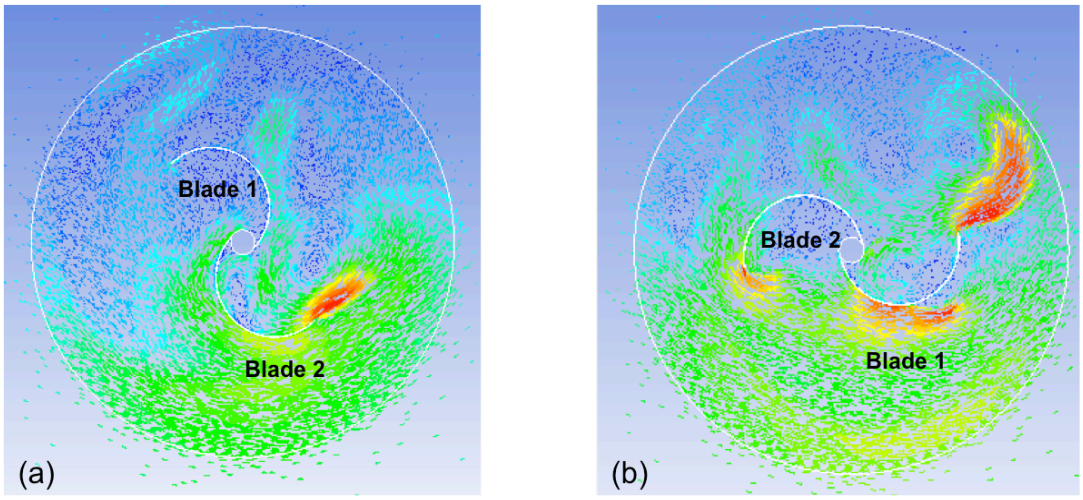

Fig. 7. Velocity vectors around a Savonius vertical axis turbine at t = 1.31s and t = 1.34s. (Blade 1 : returning blade and Blade 2 : advancing blade)

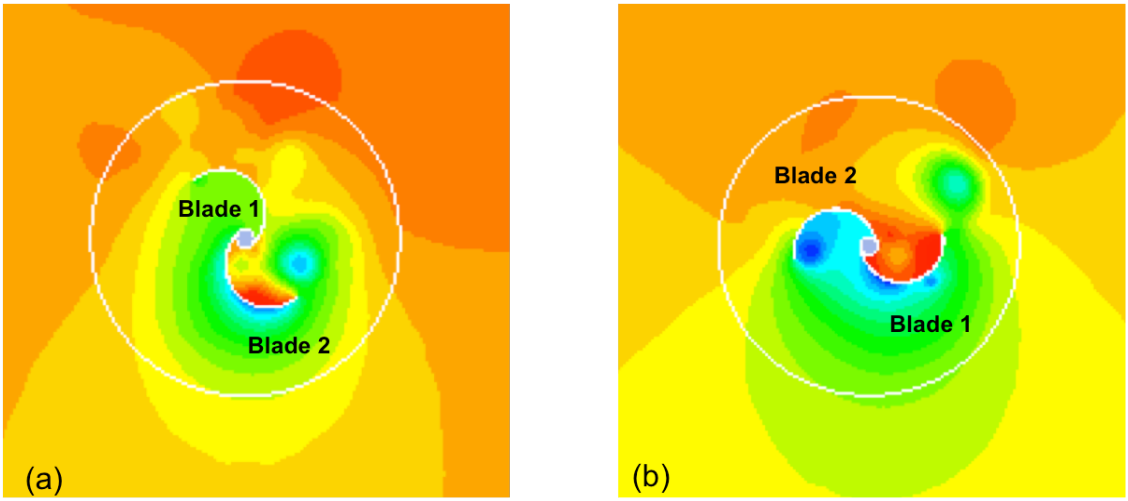

Fig. 8. Pressure distribution around a Savonius vertical axis turbine at t = 1.31s and t = 1.34s. (Blade 1 : returning blade and Blade 2 : advancing blade)

4.2. Two Savonius turbine cluster results

The efficiency of two Savonius turbines in aligned, parallel and oblique configurations is simulated and studied in this part, using different gap distances.

a Two Aligned turbines

Two aligned Savonius turbines are simulated at tip speed ratio of 0.8 and at six different gap distances (0.25D, 0.5D,

1D, 1.5D, 2D and 4D) using the same numerical method for the single Savonius turbine. Fig.9 shows an enhancement in the average power coefficient of the two aligned turbines compared to isolated Savonius turbine. The maximum average power coefficient is found to be 0.404 achieved at a gap distance equal to 4D. This maximum value represents 41.7% higher than the isolated Savonius turbine. In the case of small farm clusters and for practical reasons the choice of gap distance is limited to 4D.

b Two Parallel turbines

Two parallel Savonius turbines are simulated at tip speed ratio of 0.8 and at six different gap distances (0.25D, 0.5D, 1D, 1.5D, 2D and 2.5D) using the same numerical method for the single Savonius turbine. The numerical results in Fig.10 show an enhancement in the average power coefficient of the two parallel turbines compared to isolated turbine. The comparison shows that the maximum average power coefficient reach 0.377 achieved at a gap distance equal to 0.5D. This value represents 32% higher than the isolated turbine. The enhancement in the average power coefficient increases from 0.25D to 0.5D and then deceases as the gap distance increases.

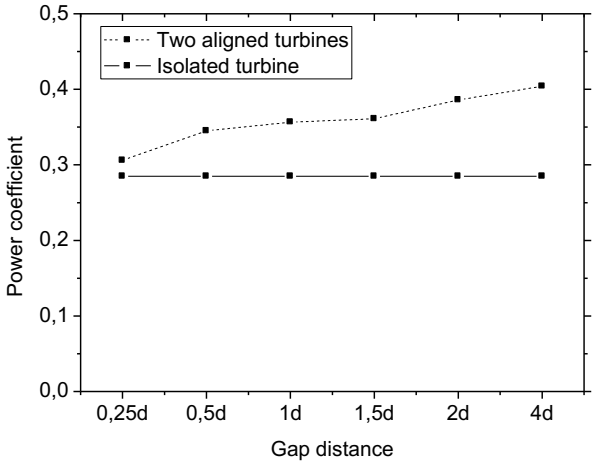

Fig.9. Average power coefficient for two aligned Savonius turbines

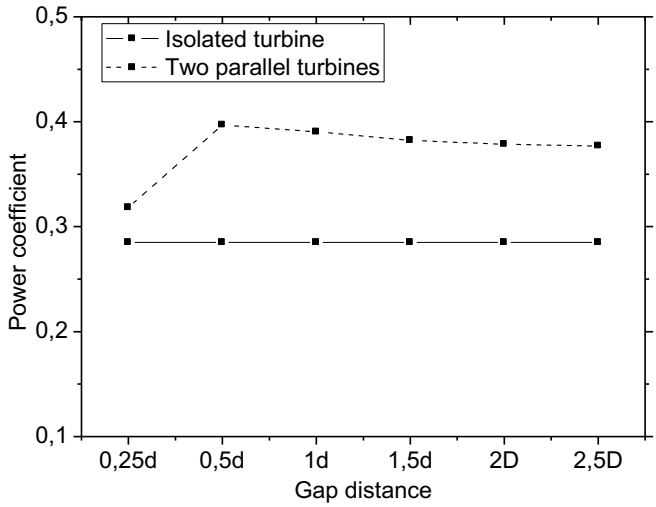

Fig.10. Average power coefficient for two parallel Savonius turbines

c Two oblique turbines

The performance of two oblique Savonius turbines are simulated and studied in forward and backward configurations compared to the principal turbine. Six different gap distances (0.25D, 0.5D, 1D, 1.5D, 2D and 2.5D) are used at a tip speed ratio of 0.8 with the same numerical method for the single Savonius turbine. In case of backward configuration, rotor (1) has the same power coefficient as an isolated rotor, an enhancement occurs in the power coefficients of rotor (2) due to the Magnus effect of rotor (1).

Table 3. Average power coefficients for the two-oblique turbine cluster, after 10 complete revolutions.

Configuration	C_p (rotor1)	C_p (rotor2)	C_p (average)
Forward	0.277	0.245	0.261
Backward	0.282	0.278	0.280

In the case of forward configuration the average power coefficient is 7.7% less than the reference value of an isolated rotor. The comparison of the average power coefficients for both configurations with the isolated turbine shows that backward configuration has higher efficiency than forward one. The average power coefficient for backward configuration is 0.280 reached at a gap distance of 0.5D as shown in Table 3. The average power coefficient decreases as the gap distance increases.

4.3 Three oblique turbine results

The performance of two parallel and oblique Savonius turbines shows that the oblique configuration is the most efficient. This result was used to develop a triangular three turbine cluster perpendicular to the wind direction. The performance of two backward oblique turbines is just 6.8% higher than two forward oblique turbines. In this part the performance of three oblique turbine clusters is studied as shown in Fig.11. The cluster consists of two forward turbines (2) and (3) as shown in Fig.11a and two backward turbines (2) and (3) as shown in Fig.11b. The numerical simulation is conducted at a tip speed ratio of 0.8 with the same numerical method for the single and two Savonius turbines. The mesh of rotating zones is refined until there is no significant change in the torque coefficient.

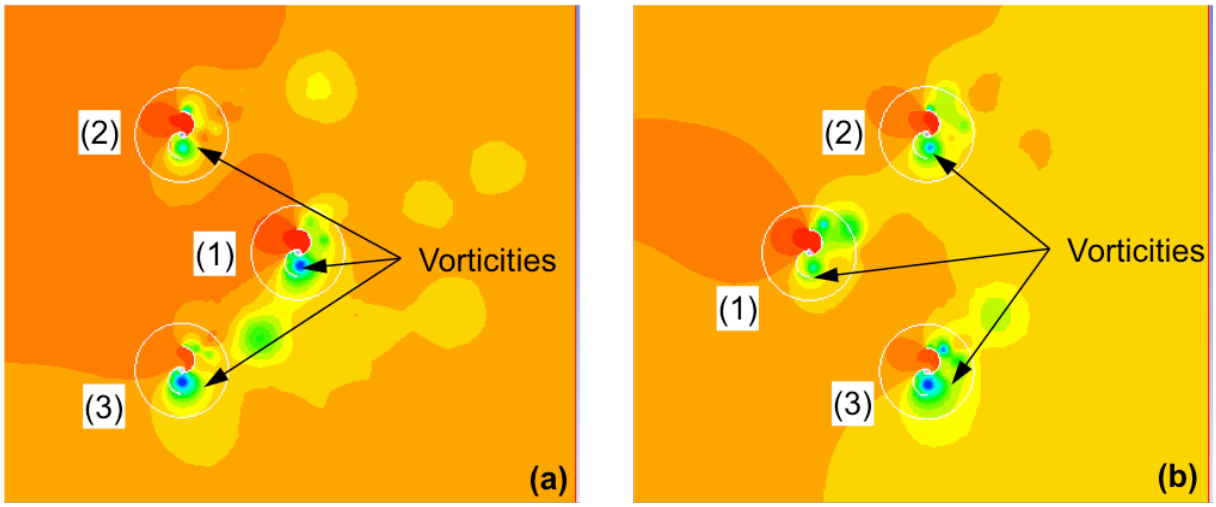

Fig. 11. Velocity distribution around three rotor Savonius turbines, after 10 revolutions.

(a) Forward configuration, (b) Backward configuration.

Table 4. Average power coefficients for the three-oblique turbine cluster, after 10 complete revolution.

Configuration	C_p (rotor1)	C_p (rotor2)	C_p (rotor3)	C_p average
Forward	0.274	0.242	0.247	0.254
Backward	0.283	0.280	0.278	0.280

The power coefficients of the three turbines are shown in Table 4. The results show an enhancement in the power coefficients of the three turbines compared to the isolated one. The total average power coefficient of the backward cluster is 0.841 and this represents about 3 times the power coefficient of an isolated turbine. The developed backward three turbines cluster generates 123 W at tip speed ratio of 0.8. The efficiency of the developed three turbine cluster is 10% higher than the forward three turbine cluster. Rotor (1) has the highest power coefficient due to the incoming higher velocity.

Conclusion :

The efficiency of a single Savonius vertical axis wind turbine, set of two aligned, parallel, forward oblique, backward oblique and triangular three cluster configurations are numerically studied for wiind energy generation. The numerical simulations for the single Savonius turbine, after 10 complete revolutions, are used for the validation of the numerical method. The results are in good agreement with experimental and numerical data coming from literature review. The assessment parameters are torque and power coefficients.

The results for the two turbine farms show an enhanced efficiency compared to single turbine. The power coefficient of backward two oblique turbines is 2 times higher than the reference value of an isolated rotor. The developed backward three turbines farm has an average power coefficient up to 6.8% higher than that of forward configuration and generates about 3 times the power coefficient of an isolated turbine. The three turbines are arranged in optimal proximity to increase their average output power and the farm topology is a geometric progression of the three turbine cluster by factor 3. This result shows that the average output power of large Savonius farms will be proportional to the number of three turbine clusters.

References

[1] G. Boroumand Jazi, B. Rismanchi, and R. Saidur, "Technical characteristic analysis of wind energy

conversion systems for sustainable development", Energy Convers Manage, Vol. 69, pp. 87–94, Mai 2013.

[2] A. Harrouz, I. Colak, and K. Kayisli, "Control of a small wind turbine system application", IEEE International Conference on Renewable Energy Research and Applications (ICRERA), pp. 1128-1133, Nov. 2016.

[3] Ö. Kiymaz, T. Yavuz, "Wind power electrical systems integration and technical and economic analysis of hybrid wind power plants", IEEE International Conference on Renewable Energy Research and Applications (ICRERA), pp. 158-163, Nov. 2016.

[4] M. Karimirad, K. Koushan, "WindWEC: Combining wind and wave energy inspired by hywind and wavestar", IEEE International Conference on Renewable Energy Research and Applications (ICRERA), pp. 96-101, Nov. 2016.

[5] M. Caruso M, A.O Di Tommaso, F. Genduso, R. Miceli, G. Ricco Galluzzo, C. Spataro, and F. Viola, "Experimental characterization of a wind generator prototype for sustainable small wind farms", IEEE International Conference on Renewable Energy Research and Applications (ICRERA), pp. 1202-1206, Nov. 2016.

[6] M. Quraan, Q. Farhat, and M. Bornat, "A new control scheme of back-to-back converter for wind energy technology", IEEE 6th International Conference on Renewable Energy Research and Applications (ICRERA), pp. 354-358, Nov. 2017.

[7] L. Kung-Yen, T. Shao-Hua, T. Chieh-Wen, and L. Huei-Jeng, "Influence of the vertical wind and wind direction on the power output of a small vertical-axis wind turbine installed on the rooftop of a building", Applied Energy, Vol. 209, pp. 383-391, Jan. 2018.

[8] S. Chaianant, U. Suchaya, C. Premchai, and L. Thananchai, "CFD-based Performance Analysis on Design Factors of Vertical Axis Wind Turbines at Low Wind Speeds", Energy Procedia, Vol. 138, pp. 500-505, Oct. 2017.

[9] N. Gabriel, P. Marius, "Parametric study of the dual vertical axis wind turbine using CFD", Journal of Wind Engineering and Industrial Aerodynamics, Vol. 172, pp. 244-255, Jan. 2018.

[10] K. Rakesh, R. Kaamran, S.F. Alan, "A critical review of vertical axis wind turbines for urban applications", Renewable and Sustainable Energy Reviews, Vol. 89, pp. 281-291, June 2018.

[11] S. Mertens, "Wind energy in urban areas: concentrator effects for wind turbines close to buildings", Refocus, Vol. 3, pp. 22-24, April 2002.

[12] B. Owens, and D. Griffith, "Aeroelastic stability investigation for large-scale vertical axis wind turbines", J. Phys.: Conf. Series, Vol. 524, 012092, 2014

[13] U.S. Paulsen, H.A. Madsen, J.H. Hattel, I. Baran, and P.H. Nielsen, "Design optimization of a 5 MW floating offshore vertical-axis wind turbine", Energy Procedia, Vol. 35, pp. 22-32, 2013.

[14] M. Borg, A. Shires, and M. Collu, "Offshore floating vertical axis wind turbines, dynamics modelling state of the art. part I", Aerodynamics Renew Sust Energ Rev, Vol. 39, pp. 1214-1225, 2014.

[15] A. Ducoin, M.S. Shadloo, and S.Roy, "Direct numerical simulation of flow instabilities over Savonius style wind turbine blades". Renew Energy, Vol. 105, pp. 374–85, 2017.

[16] S. Roy, A. Ducoin, "Unsteady analysis on the instantaneous forces and moment arms acting on a novel Savonius-style wind türbine", Energy Convers Manage, Vol. 121, pp. 281–96, August 2016.

[17] H.H. Al-Kayie, B.A. Bhayo, and M. Assadi, "Comparative critique on the design parameters and their effect on the performance of S-rotors", Renew Energy, Vol. 99, pp. 1306–1317, December 2016.

[18] A. Shigetomi, Y. Murai, Y. Tasaka, and Y. Takeda, "Interactive flow field around two Savonius turbines", Renew Energy, Vol. 36, pp. 536–545, Feb. 2011.

[19] W. Shepherd, and L. Zhang, "Electricity generation using wind power", Wold scientific publishing Co. Pte. Ltd., Singapore, 2011.

[20] J.P. Abraham, G.S. Mowry, B.P. Ploudre, E.M. Sparrow, and W.J. Minkowycz, "Numerical simulation of fluid flow around a vertical axis türbine", Journal of Renewable Sustainable Energy, Vol. 3, pp. 1-13, 2011.

[21] R. Sukanta, PhD thesis, "Aerodynamic performance evaluation of a novel savonius style wind turbine through unsteady simulations and wind tunnel experiments", 2014.

[22] R.E. Sheldahl, B.F. Blackwell, and L.V. Feltz, "Wind tunnel performance data for two- and three-bucket Savonius rotors", Sandia Report SAND 77-0131, 1977.

[23] B.D. Altan, M. Atilgan, and A. Ozdamar, "An experimental study on improvement of a Savonius rotor performance with curtaining", Exp Therm Fluid Sci, Vol. 32, pp. 1673–1678, 2008.

[24] N. Fujisawa, "On the torque mechanism of Savonius rotors", J Wind Eng Ind Aerodyn, Vol. 40, pp. 277–292, 1992.

[25] R. Sukanta, D. Ranjan, and K.S. Ujjwal, "An inverse method for optimization of geometric parameters of a Savonius- style wind türbine", Energy Conversion and Management, Vol. 155, pp. 116-127, 2018.

[26] X. Sun, D. Luo, D. Huang, and G. Wu, "Numerical study on coupling effects among multiple Savonius turbines", J Renew Sustain Energy, Vol. 4, Sep. 2012.

[27] S. Sonu, K.S. Rajesh, "Performance improvement of Savonius rotor using multiple quarter blades – A CFD investigation", Energy Conversion and Management, Vol. 127, pp. 43-54, 2016.

[28] G. Ferrari, D. Federici, P. Schito, F. Inzoli, and R. Mereu, "CFD study of Savonius wind turbine : 3D model validation and parametric analysis", Renewable Energy, Vol. 105, pp. 722-734, 2017.

[29] C.M. Chan, H.L. Bai, and D.Q. He, "Blade shape optimization of the Savonius wind turbine using a genetic algorithm", Applied Energy, Vol. 213, pp. 148-157, 2018.

[30] K.R. Sarath, P.T. Micha, S. Seralathan, and V. Hariram, "Numerical Analysis of Different Blade Shapes of a Savonius Style Vertical Axis Wind Turbine", International Journal of Renewable Energy Research, Vol.8, No.3, pp. 1654-1666, 2018.

[31] M. Shaheen, A. Shaaban, "Development of efficient vertical axis wind turbine clustered farms", Renewable and Sustainable Energy Reviews, Vol. 63, pp. 237–244, 2016.

[32] M. Shaheen, M. El-Sayed, and A. Shaaban, "Numerical study of two-bucket Savonius wind turbine cluster", J Wind Eng Ind Aerodyn, Vol. 137, pp. 78–98, 2015.

[33] H.E. Gad, A.A. Abd El-Hamid, W.A. El-Askary, and M.H. Nasef, "A New Design of Savonius Wind Turbine: Numerical Study", *CFD Letters, Vol.*6, pp. 144-158, 2014.

[34] A.M. Rafiuddin, M. Faizal, and L. Young-Ho, "Optimization of blade curvature and inter-rotor spacing of Savonius rotors for maximum wave energy extraction", Ocean Engineering, Vol. 65, pp. 32–38, 2013.

[35] V. Dossena, G. Persico, B. Paradiso, L. Battisti, S. Dell'Anna, A. Brighenti, and E. Benini, "An experimental study of the aerodynamics and performance of a vertical axis wind turbine in a confined and unconfined environment", ASME J. Energy Resour. Technol., Vol. 137, pp. 1-12, 2015.

[36] G. Persico, V. Dossena, , B. Paradiso, L. Battisti, A. Brighenti, and E. Benini, "Time-resolved experimental characterization of wakes shed by h-shaped and tro-poskien vertical axis wind turbines", ASME J. Energy Resour. Technol., Vol. 139, 1-12, 2017.

[37] P. Jaohindy, S. McTavish, F. Garde, and A. Bastide, "An analysis of the transient forces acting on savonius rotors with different aspect ratios", Renew. Energy, Vol. 55, pp. 286-295, 2013.

[38] R.E. Sheldahl, F.V. Feltz, and B.F. Blackwell, "Wind tunnel data for two and three bucket Savonius rotors", Journal of Energy, Vol. 2, pp. 160-164, 1978.

[39] M. Meziane, O. Eichwald, J.P. Sarrette, O. Ducasse, and M. Yousfi, "Multi-dimensional simulation of a polluted gas flow stressed by a DC positive multi-pins corona discharge reactor", International Journal of Plasma Environmental Science & Technology, Vol.6, pp. 98-103, 2012.

[40] M. Meziane, O. Eichwald, J.P. Sarrette, O. Ducasse, and M. Yousfi, "2D simulation of active species and ozone production in a multi-tip DC air corona discharge", The European physical journal-Applied physics, Vol. 56 (25005), pp. , 2011.

[41] H.K. Versteeg, W. Malalasekera, "An Introduction to Computational Fluid Dynamics: The Finite Volume Method", Longman Scientific & Technical, England, 1995.